JOURNAL OF THERMOPHYSICS AND HEAT TRANSFER
Vol. 6, No. 4, Oct.–Dec. 1992

Vibration-Dissociation Coupling in Nonequilibrium Flows

D. Brian Landrum* and Graham V. Candler†
North Carolina State University, Raleigh, North Carolina 27695

The nonequilibrium vibrational relaxation of a system of rotationless nitrogen molecules is simulated when instantaneously heated or cooled under constant volume and temperature constraints. A set of coupled vibrational master equations including vibration-vibration and vibration-translation exchanges, dissociation, and recombination, is numerically integrated. Exchange rates are based on Schwartz, Slawsky, and Herzfeld theory as modified by Keck and Carrier. Molecules are described by the analytic Huxley-Murrell potential. Transition rates are found to be strongly influenced by the inverse range parameter. In the heating case, transfer rates to the upper levels, reach an approximate balance with the free state resulting in a constant dissociation rate. For the cooling case, the upper levels quickly equilibrate with the free state near the translational temperature. But, these populations were significantly higher than those expected at equilibrium, signifying a population inversion. In both cases, the observed behavior is believed to be due to an inhibition of the transfer of molecules between the upper and lower vibrational levels.

Introduction

MANY proposed hypersonic vehicles would fly in the upper part of a planetary atmosphere where the low density can cause vibrational relaxation and chemical reaction rates to be of the same order as fluid convection rates. In this thermochemical nonequilibrium regime, the dissociation rate and magnitude of gas radiation are strongly affected by the vibrational state.[1] For an accurate representation of the flowfield, the thermophysical model must describe the coupling between the vibrational state and dissociation rate.

In general, when a gas is heated, the nonequilibrium vibrational distribution of diatomic molecules is formed in three identifiable stages[2]: 1) an introduction of vibrational quanta over the lowest molecular levels by the heating; 2) the introduced quanta are redistributed by collisional processes (primarily vibration-vibration (V-V) exchanges) up the vibrational "ladder" of the molecule; and 3) vibrational quanta are dissipated through gas heating by vibration-translation (V-T) relaxation or in chemical reactions such as dissociation. This finite-rate ladder-climbing process delays dissociation.

The initial focus of studies of vibration-dissociation coupling was to calculate vibrational relaxation rates. The theory of Landau and Teller[3] considered vibrational transitions between neighboring levels of a simple harmonic oscillator (SHO) and showed that the transition rates are proportional to the vibrational quantum numbers. Millikan and White[4] later correlated the vibrational relaxation time to available experimental data. A theoretical description of vibrational energy transfer by Schwartz et al.[5] (SSH theory) modeled colinear collisions between molecules and atoms or other molecules. This theory allows multilevel vibrational transitions, and molecular dissociation can be incorporated.

Early attempts to describe vibration-dissociation coupling were the coupled-vibration-dissociation (CVD) model of Hammerling et al.[6] and the preferential removal (CVDV) model of Treanor and Marrone.[7,8] These models used a simple harmonic oscillator for the molecular potential, and assumed that the vibrational degree of freedom relaxed through a series of Boltzmann distributions corresponding to the vibrational temperature T_v. Dissociation was assumed to occur from all vibrational levels with equal probability. The CVD and CVDV models do not adequately predict the inhibition of dissociation by vibrational nonequilibrium and, therefore, do not appear to embody the correct physical processes of the problem.

Currently, the most popular coupling model is the semiempirical TT_v model of Park,[9,10] that assumes that the effective dissociation rate is governed by a geometric average temperature

$$T_a = \sqrt{TT_v} \tag{1}$$

This model was chosen from an arbitrary set of candidate temperatures based on approximate reproduction of available experimental data. The model approximately predicts measured radiation characteristics of shock-heated nitrogen and air. Unfortunately, the model does not completely reproduce vibrational temperature data,[9] although more recent measurements by Sharma and Gillespie[11] lend some support to the Park model.

Sharma et al.[12] attempted to provide a theoretical basis for the TT_v model. This work used SSH theory to model transitions among all vibrational levels and to the free (dissociated) state in nitrogen. Vibrational level master equations were numerically integrated in time to recreate the relaxation process. Results for a heating case indicated a bimodal behavior for N_2 in which the upper and lower vibrational levels reach separate equilibria during relaxation. This behavior appears to be a consequence of the choice of the value for the inverse range parameter ($\alpha = 1.0 \times 10^8\ \mathrm{cm}^{-1}$), which causes a bottleneck in the exchange rates. The TT_v model approximately reproduced the calculated dissociation rate.

A recognized deficiency in the calculations of Sharma et al.[12] is the neglect of vibrational-translational energy exchange due to collisions between molecules and atoms. This exchange becomes significant for high degrees of dissociation. The correct value of the inverse range parameter is also in question. The purpose of this study is to evaluate all important physical phenomena contributing to the vibration-dissociation coupling problem. An approach similar to that of Sharma et al.[12] is used, but with several modifications to the SSH rate calculations, and inclusion of atomic collision effects. The effect of the inverse range parameter on the exchange rates is also addressed. It is hoped that this method can then be used to develop a new, more physically based model, for the dissociation and recombination rates. Such rates can then be ap-

Presented as Paper 91-0466 at the AIAA 28th Aerospace Sciences Meeting, Reno, NV, Jan. 7–10, 1991; received Feb. 2, 1991; revision received Nov. 1, 1991; accepted for publication Nov. 21, 1991.

*Research Assistant, Mechanical and Aerospace Engineering. Member AIAA.
†Assistant Professor, Mechanical and Aerospace Engineering. Member AIAA.

plied in current thermochemical nonequilibrium flowfield solution techniques.

Problem Formulation

The current study entails developing a numerical technique for the simulation of the vibrational relaxation and dissociation/recombination of N_2 in an isothermal box. This is accomplished by solving a set of coupled master equations representing the rate of change of population in each vibrational level of N_2. Both V-V and V-T exchanges between molecules and atoms are included. The effects of dissociation and recombination, to and from, each level are also included.

SSH Rate Formulation

A complete description of the development of vibrational transition rates by SSH theory is given by Clarke and McChesney.[13] The SSH theory[5] assumes one-dimensional, colinear collisions between rotationless molecules. The translational interaction potential between the two colliding molecules is approximated by an exponentially-repulsive potential

$$V(r) = V_0 e^{-\alpha r} \tag{2}$$

where r is the distance between the centers of mass of the two molecules. The V_0 and α parameters characterize the collision partners, and to a lesser extent the collision energy.

Consider a collision between two nitrogen molecules that results in the microscopic reaction

$$N_2(v_a) + N_2(v_b) \rightleftharpoons N_2(v_a') + N_2(v_b') \tag{3}$$

where one molecule transitions from vibrational level v_a to level v_a', while the collision partner transitions from v_b to v_b'. By solving the Schrödinger equation for the translational motion of a free particle in the potential field $V(r)$, Jackson and Mott[14] analytically determined the microscopic transition probability for the reaction of Eq. (3) to be

$$p_{v_a \to v_a'}^{v_b \to v_b'} = V(v_a \to v_a')^2 V(v_b \to v_b')^2 (q_f^2 - q_i^2)^2 \times \frac{\sinh(\pi q_i)\sinh(\pi q_f)}{[\cosh(\pi q_i) - \cosh(\pi q_f)]^2} \tag{4}$$

where

$$\pi q_i = \frac{4\pi^2 \mu u_i}{\alpha h}, \qquad \pi q_f = \frac{4\pi^2 \mu u_f}{\alpha h} \tag{5}$$

Here μ is the reduced mass of the collision partners, u_i and u_f are the pre- and post-collision relative velocities of the molecules, and α is the inverse range parameter defined in Eq. (2). The vibrational transition matrix elements $V(v \to v')$, are determined from the one-dimensional Schrödinger equation for vibrational motion. The transition probability of Eq. (4) accounts for both V-V and V-T exchanges by molecules. For a molecular V-T exchange $v_b = v_b'$.

The energy transferred from the translational mode to the vibrational mode is related to the vibrational level changes by the relation

$$\begin{aligned} \Delta E &= E(v_a') + E(v_b') - E(v_a) - E(v_b) \\ &= (\mu/2)(u_i^2 - u_f^2) \end{aligned} \tag{6}$$

Here $E(v)$ is the energy of vibrational level v measured from the interatomic potential minimum. When all vibrational quanta lost by one molecule are gained by the other (with no net change in their translational energies) the exchange is resonant and $\Delta E = 0$.

The microscopic probability is a function of the incident relative velocity. In a gas at translational temperature T, there are a multitude of possible initial velocities which can be assumed to be distributed according to a Maxwellian distribution. A thermally averaged transition probability is then obtained by integrating the microscopic probability over this initial (one-dimensional) velocity distribution, i.e.

$$P_{v_a \to v_a'}^{v_b \to v_b'} = \frac{\mu}{kT} \int_0^\infty u_i p_{v_a \to v_a'}^{v_b \to v_b'} \exp\left(-\frac{\mu u_i^2}{2kT}\right) du_i \tag{7}$$

A limiting form of the integral can be obtained by assuming $\pi q_i >> 1$ and $|\Delta E| >> 1$ (nonresonant transition) and using the saddle-point method. The resultant endothermic ($\Delta E > 0$) transition probability is

$$P_{v_a \to v_a'}^{v_b \to v_b'} = V(v_a \to v_a')^2 V(v_b \to v_b')^2 \left(\frac{32\pi^2 \mu kT}{\alpha^2 h^2}\right) \times f(\xi) \exp\left(-\frac{|\Delta E|}{2kT}\right)$$

$$f(\xi) = 8\sqrt{\frac{\pi}{3}}\, \xi^{7/3} \exp(-3\xi^{2/3})$$

$$\xi = \sqrt{\frac{2\pi^4 \mu (\Delta E)^2}{\alpha^2 h^2 kT}} \tag{8}$$

A bridge between nonresonant and resonant transitions was developed by Keck and Carrier.[15] When $0 \le \xi \le 21.622$ they use

$$f(\xi) = \tfrac{1}{2}\{3 - \exp[-(2\xi/3)]\}\exp[(2\xi/3)] \tag{9}$$

A similar analysis can be performed for V-T exchanges with atoms. The final thermally averaged probability is found to be

$$P_{v_a \to v_a'} = V(v_a \to v_a')^2 [(32\pi^2 \mu kT/\alpha^2 h^2)] f(\xi) \tag{10}$$

Here the forms for $f(\xi)$ are the same as in the V-V case. For this study, transition probabilities are always calculated in an endothermic manner. The reverse exothermic ($\Delta E < 0$) transition probabilities are then obtained by using the principle of detailed balance.

With the exchange probability, a rate can be written as

$$k_{v_a \to v_a'}^{v_b \to v_b'} = s\pi d_c^2 \sqrt{(8kT/\pi\mu)}\, P_{v_a \to v_a'}^{v_b \to v_b'} \tag{11}$$

where πd_c^2 is the collision cross section, d_c is the collision diameter, and s is a steric factor. For molecule-molecule collisions $d_c^2 = d_{N_2}^2$, whereas for molecule-atom collisions $d_c^2 = d_{N_2} d_N$. These values were obtained from Brokaw.[16]

In a high-temperature gas there will be molecular dissociation. It is assumed that there are various "pseudo-vibrational-levels," designated by v_c, in the continuum (free) state with energies above the dissociation energy, D_e. The maximum pseudolevel considered is 59,500 cm^{-1} above the dissociation limit. A molecule that is excited to a pseudolevel immediately decomposes into its constituent atoms. The transition is nonresonant, and the probability can be calculated by Eq. (8), but with the final vibrational level v_a' replaced by the pseudolevel v_c. Appropriate matrix elements are also substituted. A macroscopic rate for the dissociation reaction is determined by summing over all the continuum states

$$k_{v_a \to c}^{v_b \to v_b'} = \int_{E(v_c) - D_e}^{E(v_{c\max}) - D_e} k_{v_a \to v_c}^{v_b \to v_b'}\, dE \tag{12}$$

The reverse recombination rate is then found by detailed balance.

Interaction Potentials and Range Parameter

Accurate interatomic and intermolecular potentials are crucial to correctly modeling the relaxation process and associated rates. As discussed in Ref. 12, the analytic Murrell-Sorbie potential[17] is a good representation of the interatomic potential for nitrogen molecules. This potential is of the form

$$U(r) = -D_e(1 + a_1\bar{r} + a_2\bar{r}^2 + a_3\bar{r}^3)\exp(-a_1\bar{r}) \qquad \bar{r} = r - r_e \tag{13}$$

where r is the internuclear separation and r_e is the location of the potential minimum. Refinements of the potential constants ($a_1 - a_3$) were made by Huxley and Murrell[18] and are used in this study. A total of 57 bound vibrational levels (including the ground state, $v = 0$) have been determined below the dissociation limit of 79,899 cm^{-1}. All bound-bound and bound-free matrix elements and vibrational energy levels used in this study are based on the Huxley-Murrell interatomic potential.

The important effects of the intermolecular collision potential, are characterized by the inverse range parameter, α, that is a measure of molecular "hardness." This parameter appears explicitly in the transition rates based on SSH theory, and is also used in the calculation of the vibrational matrix elements $V(v_a \rightarrow v_a')$. The collision behaves more inelastically for smaller values of α, with increased probability of exchanges between the translational and vibrational modes. In a colinear collision between a molecule and another particle, the point of closest approach, or classic turning point r_c, is a function of the total collision energy $\varepsilon_\infty = \frac{1}{2}mu_i^2$. This energy can be approximated by the average kinetic energy of the heat bath. The slope of the potential and value of r_c are critical to collision behavior. These parameters are represented by the value of the inverse range parameter.

In the original SSH paper[5] α was found by matching the exponentially-repulsive potential and its slope to the Lennard-Jones potential at r_c. Using this matching process for heat bath temperatures of 4000 K $\leq T \leq$ 8000 K, a value of $\alpha = 4.7 \times 10^8$ cm^{-1} was calculated. In Ref. 12 a value of $\alpha = 1 \times 10^8$ cm^{-1} was used. Park[19] has indicated that this value was chosen, because at a particular temperature and effective collision cross section, the computed ground state transition rate was approximately that inferred from the Millikan and White correlation. Radzig and Smirnov[20] present values for α which were derived by fitting the exponentially-repulsive potential to results obtained from high energy scattering experiments. For $N_2 - N_2$ collisions, a value of $\alpha = 3.16 \times 10^8$ cm^{-1} is given whereas $\alpha = 3.31 \times 10^8$ cm^{-1} is quoted for $N_2 - N$ collisions. These values of α best characterize the intermolecular collision potential and have been used in the current work.

Master Equation Development

This study considers a collection of N_2 molecules in equilibrium at temperature T_i in a fixed volume box. The vibrational levels are populated according to a Boltzmann distribution based on the translational temperature. At time $t = 0$, the box is instantaneously heated or cooled to a new translational temperature, T_f. An isothermal condition is then maintained while collisional processes adjust the vibrational level populations to a new equilibrium distribution characteristic of T_f. If $T_f > T_i$ the upper vibrational levels will increase in population by vibrational excitation of molecules in the lower levels. Conversely, in the cooling case ($T_f < T_i$) the under-populated lower levels are increased by de-excited molecules at the expense of the upper levels. This relaxation process is further complicated by dissociation and recombination between each level, and the free or continuum state. Two cases are considered: 1) where the gas is heated from 4000 to 8000 K; and 2) where the gas is cooled from 8000 to 4000 K.

Each of the vibrational levels is modeled by a master equation that represents the temporal variation of the concentration of molecules in a level. The typical master equation for vibrational level v_a is

$$\begin{aligned}\frac{dN(v_a)}{dt} &= \sum_{v_a'} N(v_a') \sum_{v_b} N(v_b) \sum_{v_b'} k^{v_b \rightarrow v_b'}_{v_a' \rightarrow v_a} \\ &- N(v_a) \sum_{v_a'} \sum_{v_b} N(v_b) \sum_{v_b'} k^{v_b \rightarrow v_b'}_{v_a \rightarrow v_a'} \\ &+ N_a \sum_{v_a'} N(v_a') k_{v_a' \rightarrow v_a} \\ &- N_a N(v_a) \sum_{v_a'} k_{v_a \rightarrow v_a'} \\ &- N(v_a) \sum_{v_b} N(v_b) \sum_{v_b'} k^{v_b \rightarrow v_b'}_{v_a \rightarrow c} \\ &+ N_a^2 \sum_{v_b} N(v_b) \sum_{v_b'} k^{v_b \rightarrow v_b'}_{c \rightarrow v_a} \\ &- N_a N(v_a) k_{v_a \rightarrow c} + N_a^3 k_{c \rightarrow v_a}\end{aligned} \tag{14}$$

Here the $N(v)$ terms are the number densities of molecules in level v while N_a is the number density of atoms. Consider the eight terms on the right side of the equation:

1) Terms (1) and (3) represent the populating of level v_a from level v_a' due to collisions with molecules in level v_b (producing V-V exchanges) and collisions with atoms (V-T exchanges).

2) Terms (2) and (4) represent depopulation of level v_a due to the reverse of the processes described in i.

3) Terms (5) and (7) represent decreases in $N(v_a)$ by dissociation due to collisions with molecules and atoms.

4) Terms (6) and (8) represent additions to level v_a due to the three-body recombination process.

Each of the required transition rates is calculated by SSH theory as discussed above. Only transitions which involve vibrational exchanges are included in this formulation. A more complete model would also include other energy exchange processes such as rotational and electronic excitation, but is beyond the scope of this work. A discussion of the possible effects of rotation on the vibrational relaxation of hydrogen is given by Sharma and Schwenke.[21]

The full set of 57 master equations must be integrated in time. Since the actual time evolution of the relaxation process is desired, implicit methods were not considered. An explicit-Euler method was chosen for the integration that was performed on a Cray Y-MP. The code was vectorized, but run times were still significant, due to the large number of possible transitions which must be considered, and a small time step based on stability and accuracy limitations.

Results

Transition Rates and Effect of α

The value of α is based on the average translational energy of the gas molecules. Thus, each collision should be characterized by its own value of α. A calculation of α (specific to each collision) was included in a Monte Carlo simulation of the heating case by Olynick et al.[22] This was possible because of the limited number of molecules and collisions considered in particle simulations as compared to continuum calculations. For the present study, such specific calculations are numerically intractable.

There is some concern about the accuracy of the SSH rates formulated with theoretical steric factors which have often been shown to be inaccurate. Therefore, the calculated rates were corrected to match available experimental data. For the

V-V and V-T rates, the corrections are based on the $k_{0,1}$ rate, as correlated by Millikan and White.[4] This rate is based on an assumption of thermochemical equilibrium and, thus, the corresponding numerical rate must be calculated accordingly ($T_v = T_f$). The correction factor is then

$$k_{\text{corr}} = \frac{(k_{0,1})_{MW}}{(k_{0,1})_{\text{SSH},eq}} \tag{15}$$

Each microscopic rate $k^{v_b \to v_b'}_{v_a \to v_a'}$ is corrected by this factor.

For dissociation, the rate corrections are based on rate coefficients correlated to experimental data by Park,[23] which have the form (in units of cm^3 mole^{-1} s^{-1})

$$\begin{aligned} k_{d_m} &= 7 \times 10^{21} T_a^{-1.6} \exp[-(113{,}200/T_a)] \\ k_{d_a} &= 3 \times 10^{22} T_a^{-1.6} \exp[-(113{,}200/T_a)] \end{aligned} \tag{16}$$

The subscripts m and a denote rates based on collisions with molecules or atoms, respectively. Since we are interested in an equilibrium condition, $T_a = T_f$. A dissociation rate correction similar to that of Eq. (15) is then determined. Each microscopic rate $k^{v_b \to v_b'}_{v_a \to c}$ is corrected.

Figure 1 shows the initial V-V rates for single-quantum transitions from each vibrational level for the heating case. The effect of the molecular collision partner has been summed over all possible combinations of v_b and v_b'. The population of each level is that for equilibrium at T_i. The temperature dependent microscopic rates $k^{v_b \to v_b'}_{v_a \to v_a'}$ are constant since T_f is constant. The overall V-V rates change, as relaxation progresses, and the vibrational level populations evolve.

The plot illustrates the effect of the inverse range parameter, α, alluded to earlier. The first curve is for $\alpha = 1 \times 10^8$ cm^{-1} used in the calculations of Ref. 12. The two succeeding curves are for values of α derived from the Lennard-Jones potential and quoted in Ref. 20. The last curve, shows rates based on the Landau-Teller (L-T) model. Landau-Teller rates are proportional to $(v + 1)$ and, thus, increase monotonically with vibrational level. All the curves display Landau-Teller type behavior in the first four levels. For the lowest value of α, the bottleneck of Ref. 12 is evident. These rates are generally consistent with those calculated by Sharma et al.[12] except among the higher levels where a secondary minimum is not reproduced here. For the higher values of α the rate minimum is not present.

For the two highest α values, the lower half of the rates are on the order of those predicted by Landau-Teller. Upper level rates significantly exceed the L-T values. Note the large disparity in the magnitudes of the upper and lower level rates. This difference has a significant effect on the resultant vibrational relaxation. Again, the authors believe that the Radzig and Smirnov value for α is preferable, but the Lennard-Jones derived value produces rates which differ by less than an order of magnitude.

Figure 2 is a plot of the V-T rates due to collisions with atoms. There is no local minimum present for any value of α. The lowest value of α exhibits the most significant changes in the rates, in that the upper level values are approximately 11 orders of magnitude larger than those for the lower levels. As α increases, the rate magnitudes decrease, although the disparity is still significant. All values of α exhibit rates which exceed the L-T values (except in the lowest levels). Note that the V-T rates are almost identical for $\alpha = 3.16 \times 10^8$ and 4.7×10^8. Therefore, for convenience, the rates used in this study for $N_2 - N$ collisions are also based on the $N_2 - N_2$ value of α and not the value of 3.31×10^8 cm^{-1} quoted by Radzig and Smirnov.

In Fig. 3 the bound-free transition rate, $k_{VV}(v, c)$, is shown; the rate quickly increases with quantum level. The plot shows that the probability of dissociation is significant in only the uppermost 3–4 levels. The value of the inverse range parameter only slightly affects the rate magnitudes. The dissociation rates due to collisions with atoms are very similar to those of Fig. 3 (except for magnitude).

Heating Simulation

In the heating case the gas is assumed to initially be in equilibrium at $T_i = 4000$ K. The initial number density of nitrogen molecules is assumed to be $N_x = 1.0 \times 10^{17}$ cm^{-3}. Using equilibrium relations, the atomic number density is calculated to be $N_a = 7.58 \times 10^{14}$ cm^{-3}. The gas is instantaneously heated to 8000 K and allowed to relax under constant volume and temperature constraints. This process is

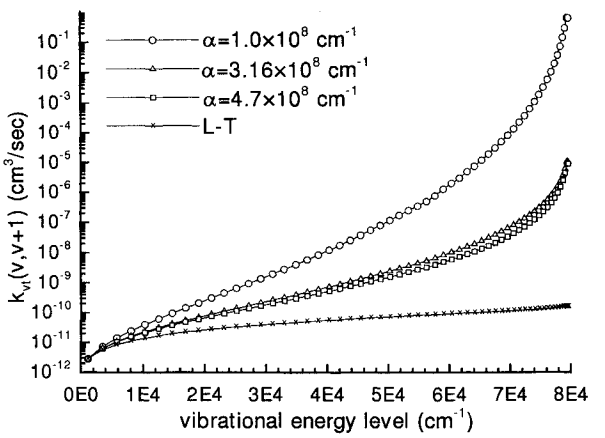

Fig. 2 Vibrational excitation rates due to collisions with nitrogen atoms as calculated by SSH theory.

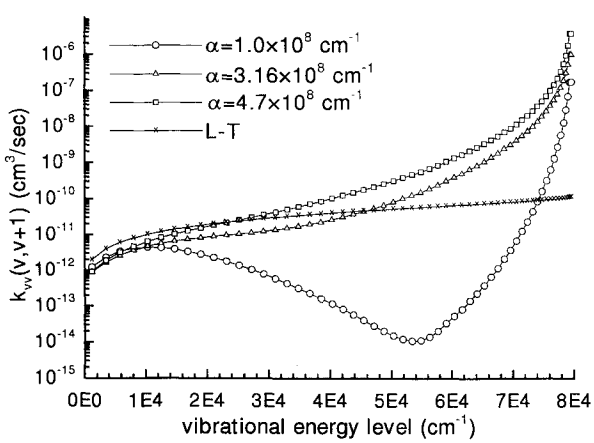

Fig. 1 Vibrational excitation rates due to collisions with N_2 molecules as calculated by SSH theory.

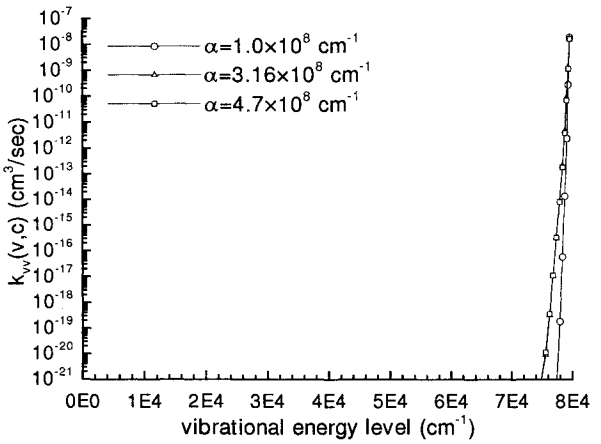

Fig. 3 Bound-free transition rates for rotationless N_2 in collision with N_2 as calculated by SSH theory.

qualitatively representative of the flow behind a normal shock wave. Results based on a value of $\alpha = 3.16 \times 10^8$ cm^{-1} are presented here. Similar results based on $\alpha = 4.7 \times 10^8$ cm^{-1} were also obtained, but will not be discussed. The master equations are integrated in time with an initial time step of 5×10^{-6} μs. This low initial value was required because of a stability limitation, and could not be increased above a value of 7×10^{-6} μs. Therefore, a significant number of computational steps were required to adequately relax the gas. Approximately 1.2×10^8 time steps and 34 h of Cray Y-MP CPU were required to calculate the heating case results shown here.

Figures 4 and 5 illustrate the relaxation process. In Fig. 4 the time evolution of the normalized population of each level $N(v)/N(v)_{eq}$ is plotted. This parameter is the number density of molecules in a given vibrational level, divided by the number density of molecules in that level at equilibrium ($T_v = T_f$). Figure 5 shows the evolution of the population of each vibrational level normalized by the total number density of molecules, N_x. When the vibrational levels are populated according to a Boltzmann distribution, the slope of the distribution is linear, and is inversely proportional to the vibrational temperature T_v (decreasing slopes represent increasing temperatures). At the first time step, the populations are represented by $T_v = 4000$ K, but the translational temperature is 8000 K. The ground state and level $v = 1$ are overpopulated for this temperature, whereas the other levels are underpopulated. Therefore, a redistribution of molecules is initiated by collisional energy exchanges. The lower levels begin to show significant changes by $t = 55.4$ μs, and appear to then relax through a series of near-Boltzmann distributions, for the rest of the simulation. A similar behavior in the lower levels was seen in the Monte Carlo study of Olynick et al.[22]

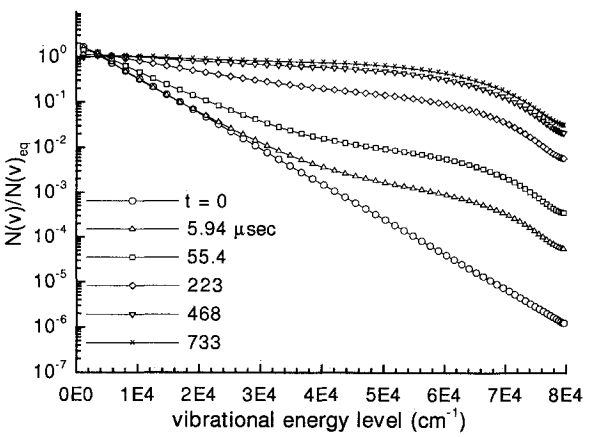

Fig. 4 Relaxation of the normalized vibrational populations. Heating case, $\alpha = 3.16 \times 10^8$ cm^{-1}.

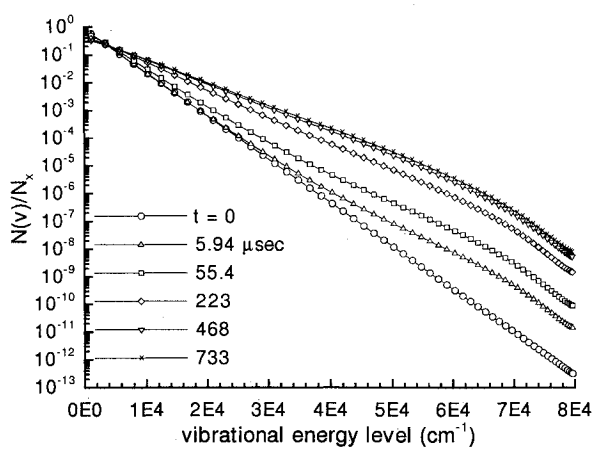

Fig. 5 Number density of each vibrational level normalized by total number of molecules. Heating case $\alpha = 3.16 \times 10^8$ cm^{-1}.

Unfortunately, due to computational constraints, the number of molecules simulated in the previous study, was too small to resolve any information about the behavior of the upper levels. By $t = 468$ μs the lowest 25 levels have nearly relaxed to equilibrium, whereas the upper levels still exhibit populations that are far from equilibrated. This distribution changes little over the rest of the simulated time. An analysis of the percentage rate of change of each level, indicates that the relative shape of the population distribution curve in the middle and upper levels, remains nearly constant throughout most of the relaxation.

The resultant lag in the upper levels can be explained by analysis of the transition rates presented in Figs. 1 and 3. There is a large disparity in the magnitude of V-V rates between the upper and lower vibrational levels. In the lower levels, the transition rates are nearly constant, while in the upper levels, they increase significantly with level. This disparity inhibits the transfer of molecules from the lowest to the highest levels. Also, only the highest levels display significant dissociation rates. Once a molecule is excited up the vibrational ladder to an upper level, the high V-V rates quickly elevate it to the highest levels where there is a high probability of dissociation. Therefore, the rate of dissociation from the upper levels is approximately balanced by the rate of molecular transfer from the lower levels.

Dissociation and recombination rates are plotted in Fig. 6. Rates due to collisions with molecules and atoms are shown separately. Dissociation rates initially increase, but then approach constants as the vibrational relaxation progresses. This is consistent with the fact that between $t = 468$ and 733 μs the absolute rates of change of the upper level populations are nearly constant with time. The final dissociation rates calculated in the simulation are $k_{dm} = 1.48 \times 10^{-16}$ and $k_{da} = 6.35 \times 10^{-16}$. The magnitudes of these calculated rates can be compared to those predicted by Eq. (16) using $T_a = \sqrt{T_t T_f}$. The resultant theoretical rates are $k_{dm} = 2.35 \times 10^{-17}$ cm^3/s and $k_{da} = 1.01 \times 10^{-16}$ cm^3/s, both of which are within an order of magnitude of the calculated values. Recombination rates plotted in Fig. 6, remain essentially constant during the relaxation simulation, which implies that they are only functions of the translational temperature.

Figure 7 is a plot of the vibrational energy per molecule and the number of free atoms vs time. It shows that vibrational equilibrium is nearly achieved before significant dissociation occurs, which agrees with experimental observations in shock heated flows. In the Sharma et al.[12] study, no atomic collisions were included, whereas, these collisions are included here. An analysis of the effects of atoms indicates that they influence the vibrational relaxation very little over the time considered. This is reasonable, since the concentration of atoms is very small, compared to that of molecules during the relaxation process, before dissociation becomes significant. The dissociation rate increases slightly when atoms are included.

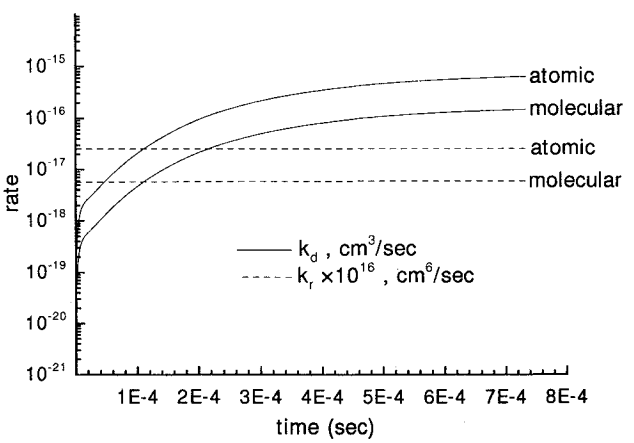

Fig. 6 Calculated dissociation and recombination rate coefficients for the vibrational relaxation of N_2. Heating case $\alpha = 3.16 \times 10^8$ cm^{-1}.

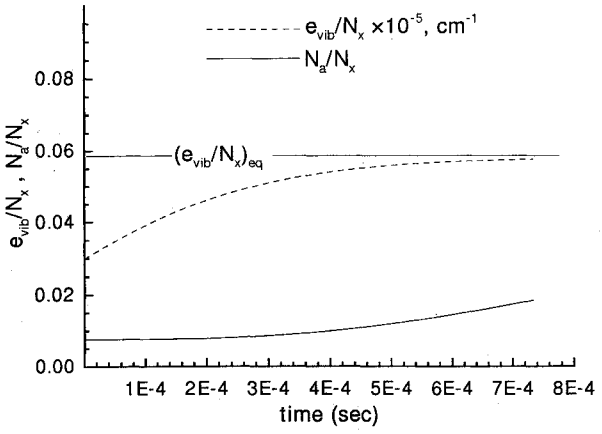

Fig. 7 Temporal variation of the vibrational energy per molecule and number of atoms. Heating case $\alpha = 3.16 \times 10^8$ cm^{-1}.

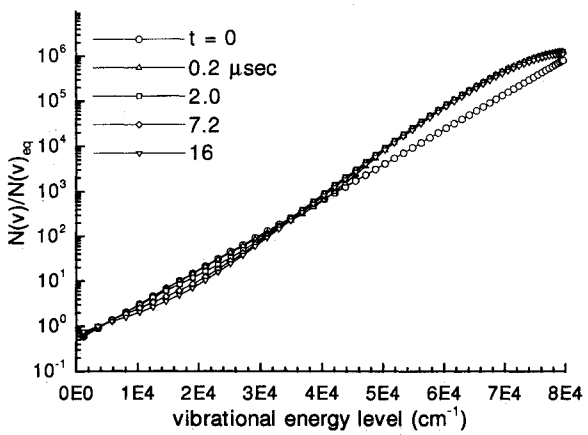

Fig. 8 Relaxation of the normalized vibrational populations. Cooling case $\alpha = 3.16 \times 10^8$ cm^{-1}.

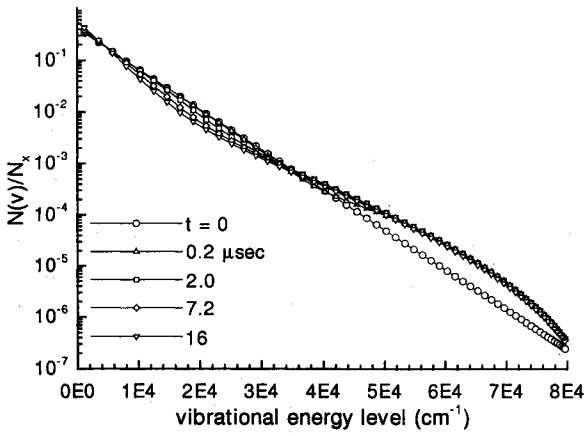

Fig. 9 Number density of each vibrational level normalized by total number of molecules. Cooling case $\alpha = 3.16 \times 10^8$ cm^{-1}.

Cooling Simulation

The simulation was next run for a cooling case where the gas was assumed to be initially in equilibrium at 8000 K. The number densities of molecules is $N_x = 1 \times 10^{17}$ cm^{-3} which yields $N_a = 8.95 \times 10^{17}$ cm^{-3}. The temperature is instantaneously dropped to 4000 K, setting up a situation where the lowest vibrational levels are underpopulated for this temperature, while the upper levels are overpopulated. Recombination should be the dominant chemical process in this case. Surprisingly, numerical simulation of this process is much more difficult than for the heating case. Stability constraints limit the maximum step size to 2×10^{-7} μs. The same value of $\alpha = 3.16 \times 10^8$ cm^{-1} used in the heating case is also used in this simulation.

In Figures 8 and 9 the normalized populations are plotted at several times. The lowest levels relax slowly toward equilibrium at 4000 K. The highest levels initially increase in population. The zero slope among the highest levels in Fig. 8 indicates that they have equilibrated with the free state near the translational temperature T_f. These populations are far above what they should be at 4000 K, signifying a population inversion. The upper levels then proceed to relax (decrease in population) while maintaining the same relative distribution. The middle level populations do not noticeably change for most of the time simulated here. An analysis of the atomic number density shows that recombination is occurring during the relaxation simulation.

Dissociation and recombination rates for the cooling case were essentially constant for the time period simulated, due to the immediate equilibration of the upper levels with the free state. Values of $k_{d_m} = 1.17 \times 10^{-14}$ cm^3/s and $k_{d_a} = 4.85 \times 10^{-14}$ cm^3/s were calculated. The results for the cooling case can be attributed to the same rate characteristics described in the heating case. Atoms recombine to form molecules that are highly excited vibrationally. These molecules are quickly redistributed among the highest vibrational levels. The disparity between the V-V rate magnitudes in the upper and lower levels, inhibits the de-excitation of molecules to the lower levels. This creates the population inversion observed.

Conclusions

A significant finding of this paper is the strong impact of the inverse range parameter α, on the vibrational exchange rates and relaxation. A low value of α produces the bottleneck seen in Ref. 12 that inhibits the transfer of vibrational energy between the lower and upper states. Using a more realistic value of α produces rates with no apparent bottleneck. In both the heating and cooling cases, the lowest vibrational levels relax slowly toward equilibrium. In the heating case, the upper levels relax to a slowly varying condition in which the rate of dissociation is approximately balanced by molecular transfer to these levels. Dissociation rates are nearly constant once the upper vibrational levels reach this state. The recombination rate is found to be a function of the translational temperature and not the vibrational distribution.

In the cooling case, the highest levels immediately increase and assume a distribution, which indicates equilibration with the free state. The populations of these levels significantly exceed the equilibrium values for the translational temperature. Thus, a population inversion is present. The resultant dissociation rates are constant throughout the time simulated.

Acknowledgments

Support for this work was provided by NASA Ames Research Center under Cooperative Agreement No. NCA2-519 and by NASA Grant No. NAGW-1331 to the Mars Mission Research Center at North Carolina State University. Mr. Landrum was also supported by a National Defense Science and Engineering Graduate fellowship sponsored by the Air Force Office of Scientific Research, Bolling AFB, DC. Computer time was provided by the North Carolina Supercomputing Center. The authors thank S. P. Sharma, W. M. Huo, and C. Park for providing the vibrational matrix element programs and insight into the SSH formulation.

References

[1]Howe, J. T., "Introductory Aerothermodynamics of Advanced Space Transportation Systems," *Journal of Spacecraft and Rockets*, Vol. 22, No. 1, 1985, pp. 19–26.

[2]Capitelli, M. (ed.), "Topics in Current Physics 39," *Nonequilibrium Vibrational Kinetics*, Springer-Verlag, Berlin, 1986, p. 2.

[3]Landau, L., and Teller, E., "Theory of Sound Dispersion," *Phy-*

sikalische Zeitschrift der Sowjetunion, Vol. 10, 1936, pp. 34–43.

[4]Millikan, R. C., and White, D. R., "Systematics of Vibrational Relaxation," *Journal of Chemical Physics*, Vol. 39, No. 12, 1963, pp. 3209–3213.

[5]Schwartz, R. N., Slawsky, Z. J., and Herzfeld, K. F., "Calculation of Vibrational Relaxation Times in Gases," *Journal of Chemical Physics*, Vol. 20, No. 10, 1952, pp. 1591–1599.

[6]Hammerling, P., Teare, J. D., and Kivel, B., "Theory of Radiation from Luminous Shock Waves in Nitrogen," *Physics of Fluids*, Vol. 2, No. 4, 1959, pp. 422–426.

[7]Treanor, C. E., and Marrone, P. V., "Effect of Dissociation on the Rate of Vibrational Relaxation," *Physics of Fluids*, Vol. 5, No. 9, 1962, pp. 1022–1026.

[8]Marrone, P. V., and Treanor, C. E., "Chemical Relaxation with Preferential Dissociation from Excited Vibrational Levels," *Physics of Fluids*, Vol. 6, No. 9, 1963, pp. 1215–1221.

[9]Park, C., "Assessment of Two-Temperature Kinetic Model for Dissociating and Weakly-Ionizing Nitrogen," AIAA Paper 86-1347, 1986.

[10]Park, C., "Assessment of Two-Temperature Kinetic Model for Ionizing Air," AIAA Paper 87-1574, 1987.

[11]Sharma, S. P., and Gillespie, W., "Nonequilibrium and Equilibrium Shock Front Radiation Measurements," AIAA Paper 90-0139, 1990.

[12]Sharma, S. P., Huo, W. M., and Park, C., "The Rate Parameters for Coupled Vibration-Dissociation in a Generalized SSH Approximation," AIAA Paper 88-2714, 1988.

[13]Clarke, J. F., and McChesney, M., *Dynamics of Relaxing Gases*, Chap. 3, Butterworths, London, 1976.

[14]Jackson, J. M., and Mott, N. F., *Proceedings of the Royal Society of London, Series A*, No. 137, 1932, p. 703.

[15]Keck, J., and Carrier, G., "Diffusion Theory of Nonequilibrium Dissociation and Recombination," *Journal of Chemical Physics*, Vol. 43, No. 7, 1965, pp. 2284–2298.

[16]Brokaw, R. S., "Energy Transport in High Temperature and Reacting Gases," *Planetary and Space Science, Proceedings of the Conference on Physical Chemistry in Aerodynamics and Space Flight*, edited by M. Green, Pergamon, Vol. 3, 1961, pp. 238–252.

[17]Murrell, J. N., and Sorbie, K. S., "New Analytic Form for the Potential Energy Curves of Stable Diatomic States," *JCS Faraday Transactions II*, Vol. 70, 1974, pp. 1552–1556.

[18]Huxley, P., and Murrell, J. N., "Ground-State Diatomic Potentials," *JCS Faraday Transactions II*, Vol. 79, 1983, pp. 323–328.

[19]Park, C., private communication.

[20]Radzig, A. A., and Smirnov, B. M., *Reference Data on Atoms, Molecules, and Ions*, Springer Series in Chem. Phys. 31, Springer-Verlag, Berlin, 1985.

[21]Sharma, S. P., and Schwenke, D. W., "The Rate Parameters for Coupled Rotation-Vibration-Dissociation Phenomenon in H_2," AIAA Paper 89-1738, 1989.

[22]Olynick, D., Moss, J., and Hassan, H., "Monte Carlo Simulation of Vibrational Relaxation in Nitrogen," AIAA Paper 90-1767, 1990.

[23]Park, C., "Two-Temperature Interpretation of Dissociation Rate Data for N_2 and O_2," AIAA Paper 88-0458, 1988.